Deformation and Cyclic Strength Characteristics of Loose and Medium-Dense Clean Sand under Sloping Ground Conditions: Insights from Cyclic Undrained Torsional Shear Tests with Static Shear

G. Chiaro[1], M. Umar[2], T. Kiyota[2], and J. Koseki[3]
[1]*Department of Civil and Natural Resources Engineering, University of Canterbury, Christchurch, New Zealand*
[2]*Institute of Industrial Science, University of Tokyo, Tokyo, Japan*
[3]*Department of Civil Engineering, University of Tokyo, Tokyo, Japan*
E-mail: gabriele.chiaro@canterbury.ac.nz

ABSTRACT: The effects of liquefaction on sloping ground often include the development of extremely large deformation. Although such phenomenon has been repeatedly observed following major earthquakes, the triggering conditions are not fully understood yet. To provide new insights into this issue, in this paper, results of two series of large-strain undrained cyclic torsional shear tests with initial static shear conducted on loose and medium-dense Toyoura sand specimens (relative density of 25-30% and 44-48%) are presented and analyzed. The post-liquefaction response of Toyoura sand is assessed in terms of failure modes and cyclic resistance up to 50% single amplitude shear strain. It is shown that, depending on the combined magnitude of static and cyclic shear stresses, a sand in sloping ground will likely experience a sudden development of large shear deformation (flow deformation) if initial liquefaction takes place, or a more progressive accumulation of large residual deformation, which yet may bring sand to failure, when the onset of initial liquefaction is not achieved.

KEYWORDS: Flow deformation, Liquefaction, Residual deformation, Shear failure, Simple shear, Sloping ground.

1. INTRODUCTION

Soil liquefaction is a phenomenon that typically occurs in saturated loose sandy soils during earthquakes. Its effects are most evident in sloping ground, where the liquefaction-induced substantial loss of soil shear strength and stiffness results typically in very large lateral ground displacement. The phenomenon and field manifestation associated with such lateral ground deformation is commonly referred to as flow failure or flow deformation. While the consequences of liquefaction (e.g. damage to piles and access of bridges, roads, flood-prevention systems and riverbanks, embankment dams, landslides etc.) have been well documented during recent earthquakes (e.g. Cubrinovski et al., 2010, 2011; Kiyota et al., 2011; Chiaro et al., 2015b, 2017a, 2018), there is still a lack of knowledge as to the mechanics for flow deformation (triggering and driving forces, large shear strain development characteristics and shear strength recovery process) in liquefied sandy soils. This limits our ability to identify susceptible soil in advance and thus prevent potential catastrophic failures from occurring.

In any seismic event, large ground deformation represents a major hazard to many engineering structures and buried lifeline facilities. Therefore, when evaluating liquefaction, it is important to assess whether or not a given soil in its in-situ density-stress state has the potential for flow failure (Verdugo and Ishihara, 1996; Cubrinovski and Ishihara, 2000). However, this is not an easy task, since flow failure is a complex phenomenon governed by many interdependent factors such as sloping ground conditions, earthquake characteristics (shear stress amplitude and number of cycles), confining stress level and soil density among others (Yoshimi and Oh-oka, 1975; Castro and Poulus, 1977; Vaid and Finn, 1979; Tatsuoka et al., 1982; Vaid and Chern, 1983; Hyodo et al., 1991, 1994; Vaid et al., 2001; Yang and Sze, 2011a, 2011b; Sivathayalan and Ha, 2011; Chiaro et al., 2012, 2013a, 2013b, 2017b; Ziotopoulou and Boulanger, 2016).

Laboratory element tests enable evaluation of soil behaviour under well-defined density-stress conditions. However, commonly used triaxial devices fail to reproduce realistic stress conditions and soil deformation modes (Chiaro et al., 2013a). Conversely, technical limitations prevent the simulation of strains larger than 10-15% using conventional simple shear devices (Cappellaro et al., 2018). Thus, the majority of test results presented to date are inadequate for quantifying the effects of the interdependent density-stress factors on flow deformation. On the other hand, torsional shear apparatus on hollow cylindrical specimens is recognized as an excellent tool to properly evaluate liquefaction soil response (Tatsuoka et al., 1982; Arangelovski and Towhata, 2004; Georgiannou et al., 2008). In particular, it allows to reproduce the simple shear conditions (Koseki et al., 2005) and achieve single amplitude shear strain exceeding 50% (Kiyota et al., 2008). Accordingly, with the aim of addressing the uncertainty before mentioned, Chiaro et al. (2012, 2013a) performed a number of large-strain cyclic undrained torsional simple shear tests with initial static shear on medium-dense Toyoura sand specimens (D_r = 44-48%). It was confirmed that the presence of initial static shear does play a key role on the failure modes of sand in sloping ground (i.e. flow failure or shear failure), the way shear strain level can developed (i.e. flow deformation or progressive deformation accumulation) and the extend of residual deformation. However, no experimental data from cyclic undrained torsional shear tests with initial static shear are available for other relative density values.

In view of the above background and to provide new insights into the mechanisms for flow deformation and cyclic resistance of saturated sand in sloping ground subjected to undrained cyclic shear loading, in this paper, the test results presented in Chiaro et al. (2012, 2013a) are re-analysed and supplemented with new experimental evidences obtained for loose Toyoura sand specimens (D_r = 25-30%) subjected to single amplitude shear strain up to 50% under various combinations of static shear and cyclic shear stresses (i.e. stress-reversal and no-stress-reversal loading conditions).

2. TEST APPARATUS, MATERIAL AND PROCEDURE

2.1 Torsional Shear Apparatus

In this study, to achieve single amplitude torsional shear strain levels exceeding 50%, the torsional shear apparatus on hollow cylindrical specimens shown in Figure 1 was employed. The torque and axial loads were detected by using a two-component load cell, which is installed inside the pressure chamber. Difference in pressure levels between the cell pressure and the pore water pressure was measured by a high-capacity differential pressure transducer (HCDPT). Volume change during the consolidation process was measured by a low-capacity differential pressure transducer (LCDPT). A potentiometer with a wire and a pulley was employed to measure the rotation angle of the top cap and, thus, the torsional shear strains. The loading system was controlled by a computer (via a feedback-loop set onto the force readings from the load cell and the rotation angle from the potentiometer) that computes the stresses and strains applied on the soil specimen and in real-time controls the device.

As illustrated in Figure 2, the hollow cylinder torsional shear apparatus allows independent control of four loading components (Figure 2), namely vertical axial load (F_z), torque load (T), inner cell pressure (p_i) and outer cell pressure (p_o). The correspondent stress components (i.e. axial stress (σ_z), radial stress (σ_r), circumferential stress (σ_θ) and torsional shear stress ($\tau_{z\theta}$)) were calculated as Hight et al. (1983):

$$\sigma_z = \frac{F_z}{\pi(r_o^2 - r_i^2)} + \frac{(p_o r_o^2 - p_i r_i^2)}{(r_o^2 - r_i^2)} \quad (1)$$

$$\sigma_r = \frac{(p_o r_o + p_i r_i)}{(r_o + r_i)} \quad (2)$$

$$\sigma_\theta = \frac{(p_o r_o - p_i r_i)}{(r_o - r_i)} \quad (3)$$

$$\tau = \tau_{z\theta} = \frac{3T}{2\pi(r_o^3 - r_i^3)} \quad (4)$$

where r_o and r_i are the outer and inner radii of the specimen, respectively.
The average torsional shear strain was computed as:

$$\gamma = \gamma_{z\theta} = \frac{2\theta\,(r_o^3 - r_i^3)}{3H\,(r_o^2 - r_i^2)} \quad (5)$$

where θ is the circumferential angular displacement and H is the specimen height.

The average principal stresses σ_1 (major), σ_2 (intermediate), σ_3 (minor) and the mean principal stress p were given by:

$$\begin{Bmatrix}\sigma_1\\ \sigma_3\end{Bmatrix} = \frac{\sigma_z + \sigma_\theta}{2} \pm \sqrt{\left(\frac{\sigma_z - \sigma_\theta}{2}\right)^2 + \tau_{z\theta}^2} \quad (6)$$

$$\sigma_2 = \sigma_r \quad (7)$$

$$p = \frac{\sigma_1 + \sigma_2 + \sigma_3}{3}; \qquad p' = p - u \quad (8)$$

where p' is the effective mean stress and u is the pore water pressure.

It should be noted that, in this study, p_i and p_o were kept equal to each other. Moreover, the measured shear stress and mean effective stress were corrected for the effects of the membrane force.

2.2 Material, Specimen Preparation and Test Procedure

All the tests were performed on Toyoura sand, which is a uniform quartz sand with sub-angular particle shape and negligible fines content (G_s = 2.656; e_{max} = 0.992; e_{min} = 0.632; F_c = 0.1%). Its gradation curve and an optical microscope photo showing the typical particle shape are shown in Figure 3.

Several medium-size hollow cylindrical specimens with dimension of 150 mm in outer diameter, 90 mm in inner diameter and 300 mm in height were prepared by air pluviation method at a relative density (D_r) of 25-30% and 44-48%. To minimize the degree of inherent anisotropy in the radial direction of hollow cylindrical sand specimens, specimen preparation was carried out by carefully pouring air-dried sand particles into a mold while moving radially and at the same time circumferentially in alternative directions (i.e. first in clockwise and then anti-clockwise directions) the nozzle of the pluviator (De Silva et al., 2015). To achieve specimens with highly uniform density, the falling height of sand grains was kept constant throughout the pluviation process. To assure a high degree of saturation: the double vacuum method (Ampadu, 1991) was first employed; then, de-aired water was circulated into the specimens; and, finally, a back pressure of 200 kPa was applied. Skempton's B-value ≥ 0.96 was measured for all the tested specimens.

After saturation, specimens were isotropically consolidated by increasing the effective mean stress to 100 kPa. Subsequently, a specific value of initial static shear was applied by drained monotonic torsional shearing, which replicates the gravitational shear stress component induced by slope inclination. Finally, to replicate seismic loading conditions, uniform cycles of undrained cyclic torsional shear stress amplitude were applied at a shear strain rate of 2.5%/min. The loading direction was reversed when the amplitude of shear stress reached the target value. During the process of undrained cyclic torsional loading the vertical displacement of the top cap was prevented with the aim to simulate as much as possible the simple shear conditions that ground undergoes during horizontal excitation (Kiyota et al., 2008).

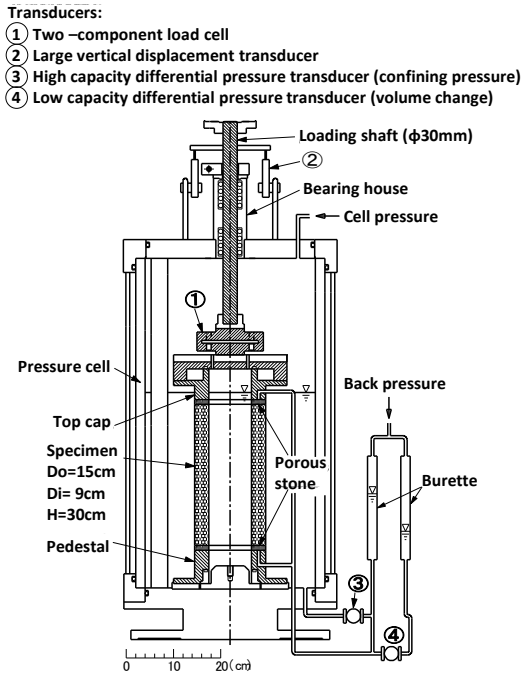

Figure 1 Torsional shear apparatus on hollow cylindrical specimens used in this study (Kiyota et al., 2008)

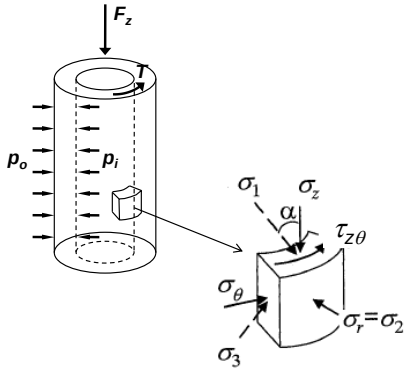

Figure 2 External forces and stress components acting on a hollow cylindrical specimen (Chiaro et al., 2013b and 2017b)

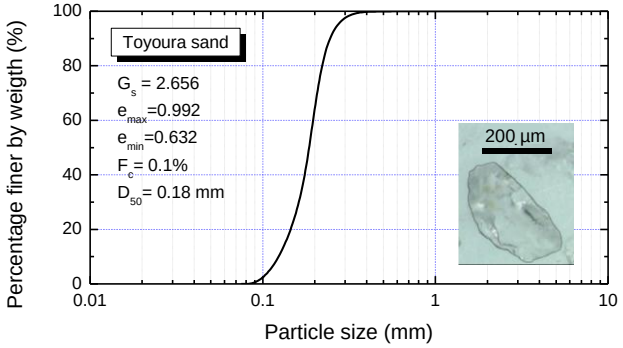

Figure 3 Particle size distribution and grain shape of Toyoura sand

2.3 Stress-Reversal and No-Stress-Reversal Loading Conditions

As described schematically in Figure 4, before earthquake shaking, a soil element beneath sloping ground is subjected to an initial static shear stress (τ_{static}) induced by the slope inclination conditions. During earthquake shaking, the reference soil element undergoes partial or no shear stress reversal loading conditions due to the superimposition of seismically-induced cyclic shear stress (τ_{cyclic}) to τ_{static}. When $\tau_{static} < \tau_{cyclic}$, the shear stress changes within the maximum positive value τ_{max} ($= \tau_{static} + \tau_{cyclic}$) > 0 and the minimum negative value τ_{min} ($= \tau_{static} - \tau_{cyclic}$) < 0 during each cycle of loading. This type of loading is known as stress-reversal or two-way loading. On the other hand, when $\tau_{static} > \tau_{cyclic}$, the shear stress is always positive (i.e. $\tau_{max} > 0$ and $\tau_{min} > 0$). This condition is called no-stress-reversal or one-way loading (Yoshimi and Oh-oka, 1975; Hyodo et al., 1991).

In view of the above, in this study, the influence of stress-reversal and no-stress-reversal was investigated by considering various combinations of τ_{static} and τ_{cyclic}. Tests were carried out over a range of τ_{static} varying from 0 to 30 kPa and three levels of τ_{cyclic} (i.e. 12, 16 and 20 kPa), as listed in Table 1.

3. TEST RESULTS AND DISCUSSIONS

3.1 Membrane Force Corrections

Koseki et al. (2005) pointed out that in performing torsional shear tests on hollow cylindrical soil specimens, due to the presence of inner and outer membranes, the effect of membrane force on measured torsional shear stress cannot be neglected (i.e. to calculate the shear stress effectively applied on the soil specimen, the total stress measured by the load cell needs to be corrected for the apparent shear stress induced by the presence of the membrane). In a similar manner, the mean effective stress requires amendments due to membrane force effects as well (Chiaro et al., 2013a). Usually, the membrane force is computed based on the linear elasticity theory, which assumes cylindrical deformation of specimen. Nevertheless, experimental evidences clearly demonstrate that at large shear strains, deformation of a hollow cylindrical sand specimen is not uniform along the specimen height and specimen shape is far from being perfectly cylindrical (Kiyota et al., 2008; Chiaro et al., 2013a). To experimentally evaluate the membrane force a specific testing procedure was developed by Kiyota et al. (2008), which consists of shearing a hollow cylindrical water specimen from small to large shear strain levels in the torsional shear apparatus.

As shown in Figure 5, in this study, the measured shear stress was corrected for the effect of membrane force by employing the most recent empirical hyperbolic correlation between the apparent shear stress due to membranes (τ_m) and the shear strain (γ) reported by Chiaro et al. (2017c). The effective mean principal stress was corrected by using the linear expression between the apparent vertical stress due to membranes ($\sigma_m/3$) and the shear strain (γ), which was derived from experimental data from Chiaro et al. (2013a).

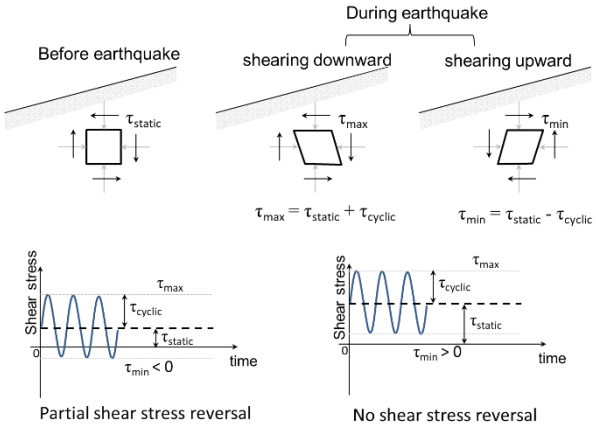

Figure 4 Stress conditions in sloping ground during earthquakes (Chiaro et al., 2017b)

3.2 Failure Mechanisms and Large Deformation Development

In this section, typical test results are presented for loose Toyoura sand in terms of stress-strain relationships, effective stresses paths and excess pore water pressure (EPWP) generation response. Three distinct deformation modes that loose sand in sloping ground may experience during earthquakes are identified: i) potential development of flow deformation due to cyclic liquefaction; ii) abrupt development of flow deformation due to rapid (flow) liquefaction, and iii) progressive accumulation of residual deformation inducing shear failure. Note that the results for medium dense Toyoura sand have already been exhaustively reported in Chiaro et al. (2012, 2013a) and, therefore, will not be described in this paper in terms of failure mechanisms.

Table 1 Undrained cyclic torsional shear tests analyzed in this study

Test	D_r (%)	τ_{cyclic} (kPa)	τ_{static} (kPa)	Loading type	Reference
1	30	12	0	Reversal	This study
2	28	12	5	Reversal	
3	26	12	10	Reversal	
4	26	12	15	No-Reversal	
5	25	12	20	No-Reversal	
6	28	12	25	No-Reversal	
7	25	12	30	No-Reversal	
8	25	16	0	Reversal	This study
9	26	16	5	Reversal	
10	26	16	10	Reversal	
11	30	16	15	Reversal	
12	28	16	20	No-Reversal	
13	29	16	25	No-Reversal	
14	46	16	0	Reversal	Chiaro et al. (2012, 2013a)
15	46	16	5	Reversal	
16	47	16	10	Reversal	
17	44	16	15	Reversal	
18	45	16	20	No-Reversal	
19	48	20	0	Reversal	Chiaro et al. (2012, 2013a)
20	48	20	5	Reversal	
21	46	20	10	Reversal	
22	44	20	15	Reversal	
23	47	20	20	Reversal	
24	46	20	25	No-Reversal	
Effective mean principal stress, $p_0' \approx 100$ kPa					

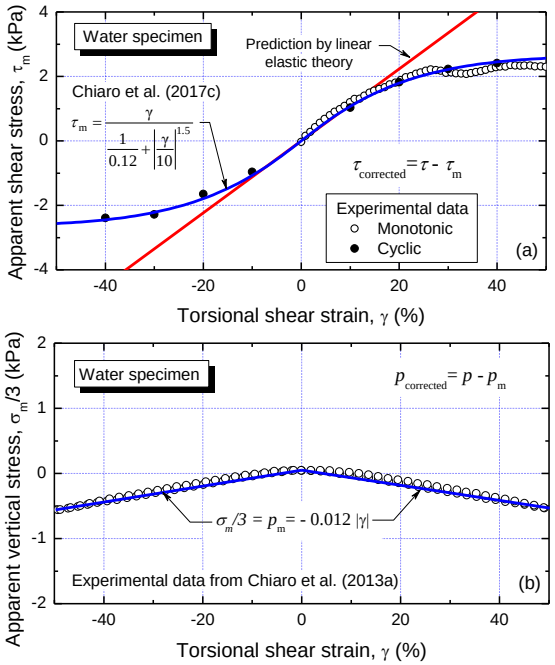

Figure 5 Membrane force corrections used in this study

3.2.1 Potential Development of Flow Deformation

Figures 6 and 7 show the results of Test 2 (stress-reversal; D_r = 28%; τ_{static} = 5 kPa; τ_{cyclic} = 12 kPa) and Test 9 (stress-reversal; D_r = 26%; τ_{static} = 5 kPa; τ_{cyclic} = 16 kPa). In both tests, a gradual EPWP generation besides a negligible shear strain development is observed until the initial liquefaction state ($r_u = p'/p_0' = 100\%$) is reached. After this point (i.e. post-liquefaction stage), a sudden development of large shear strain exceeding 50% is observed. This type of undrained cyclic response, which potentially may induce large post-liquefaction flow deformation, is referred to as cyclic mobility (Yang and Sze, 2011a) or cyclic liquefaction (Chiaro et al., 2012) and is commonly observed in loose/medium dense sand exhibiting a limited strain softening behavior (i.e. no flow-type static liquefaction failure) under monotonic undrained shearing.

From a practical viewpoint, under realistic earthquake conditions, cyclic liquefaction would take place and trigger flow deformation only if an earthquake produces a substantial number of cycles with large shear stress amplitude. For instance, if a reference moment magnitude (M_w) 7.5 earthquake is considered, then it is expected that it will induce not more than 15 shear stress cycles of uniform amplitude (Seed and Idriss, 1982). Thus, as shown in Figure 6(c), under the stress conditions considered in Test 3, although the sand has the potential to liquefy, initial liquefaction (r_u = 100%) will not take place and large extent of strains will not develop within 15 cycles. On the other hand, as shown in Figure 7(c), under the stress conditions used in Test 9, initial liquefaction will be achieved in less than 15 loading cycles, and a consequent sudden development of extremely large shear strain can be expected during the cyclic mobility phase.

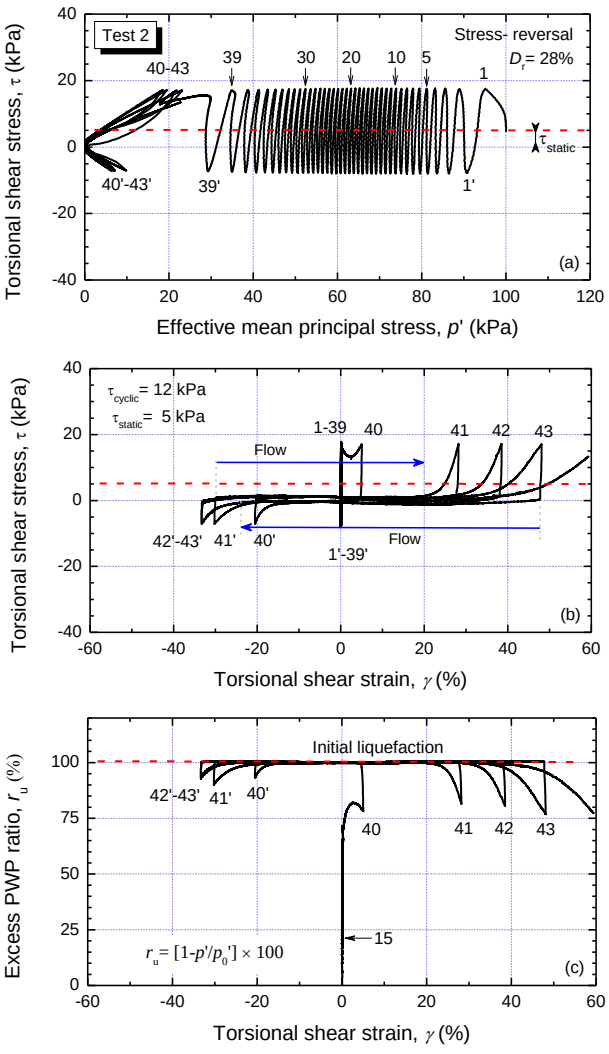

Figure 6 Cyclic liquefaction response with no occurrence of flow deformation within 15 cycles

3.2.2 Abrupt Development of Flow Deformation

In contrast to the previous case, as shown in Figure 8, in Test 11 (stress-reversal; D_r = 30%; τ_{static} = 15 kPa; τ_{cyclic} = 16 kPa) an immediate and substantial EPWP build-up is observed (i.e. the condition of initial liquefaction (r_u = 100%) is attained during the first loading cycle). This is followed by the rapid development of large shear strain exceeding 50% in less than 4 cycles. This type of undrained cyclic response is referred to as flow-type failure (Yang and Sze, 2011a) or rapid (flow) liquefaction (Chiaro et al., 2012), and similarly to the case previously examined, is also commonly observed in loose/medium dense sand exhibiting a stable behavior under monotonic undrained loading.

The above described flow-type liquefaction behavior can be easily activated by a strong earthquake with moment magnitude of M_w 7 to M_w 8, which corresponds to 10 to 20 uniform cycles of large shear stress amplitude.

3.2.3 Shear Failure due to Accumulation of Residual Deformation

For Test 12 (no-stress-reversal; D_r = 28%; τ_{static} = 20 kPa; τ_{cyclic} = 16 kPa), shown in Figure 9, although the initial EPWP generation and limited flow deformation remained similar to those seen in Test 11, flow-type failure did not occur. Because the nearly-zero effective stress state was temporary, the associated strain softening did not produce failure. Instead, as the loading progressed the soil regained its strength and stiffness as a result of dilation. This behavior repeated itself in the subsequent cycles, accompanied by a steady EPWP response. The soil kept deforming due to the accumulation of large residual shear strain that eventually brought the specimen to failure.

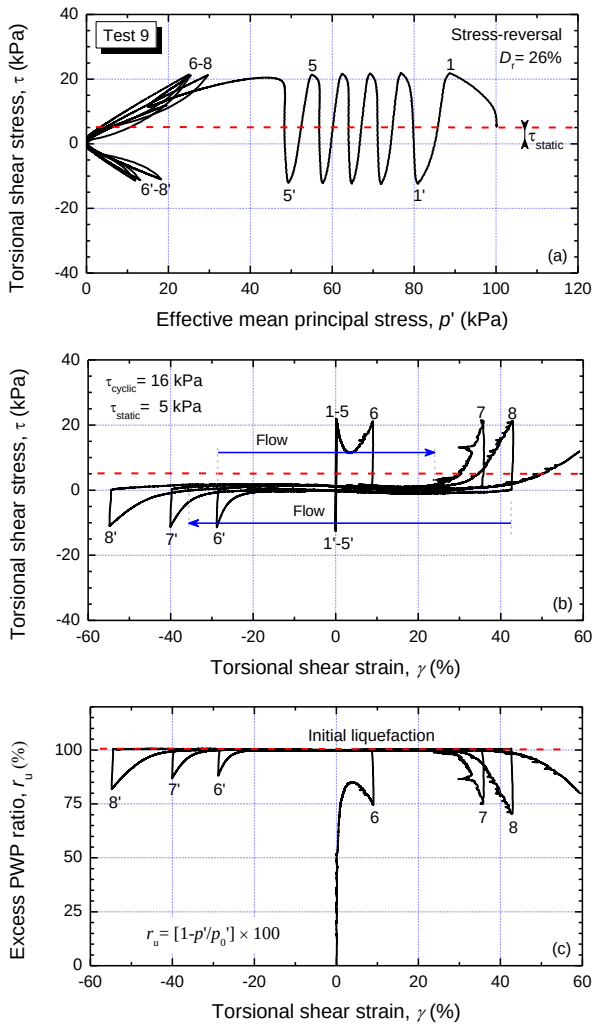

Figure 7 Cyclic liquefaction response with the occurrence of flow deformation in less than 15 cycles

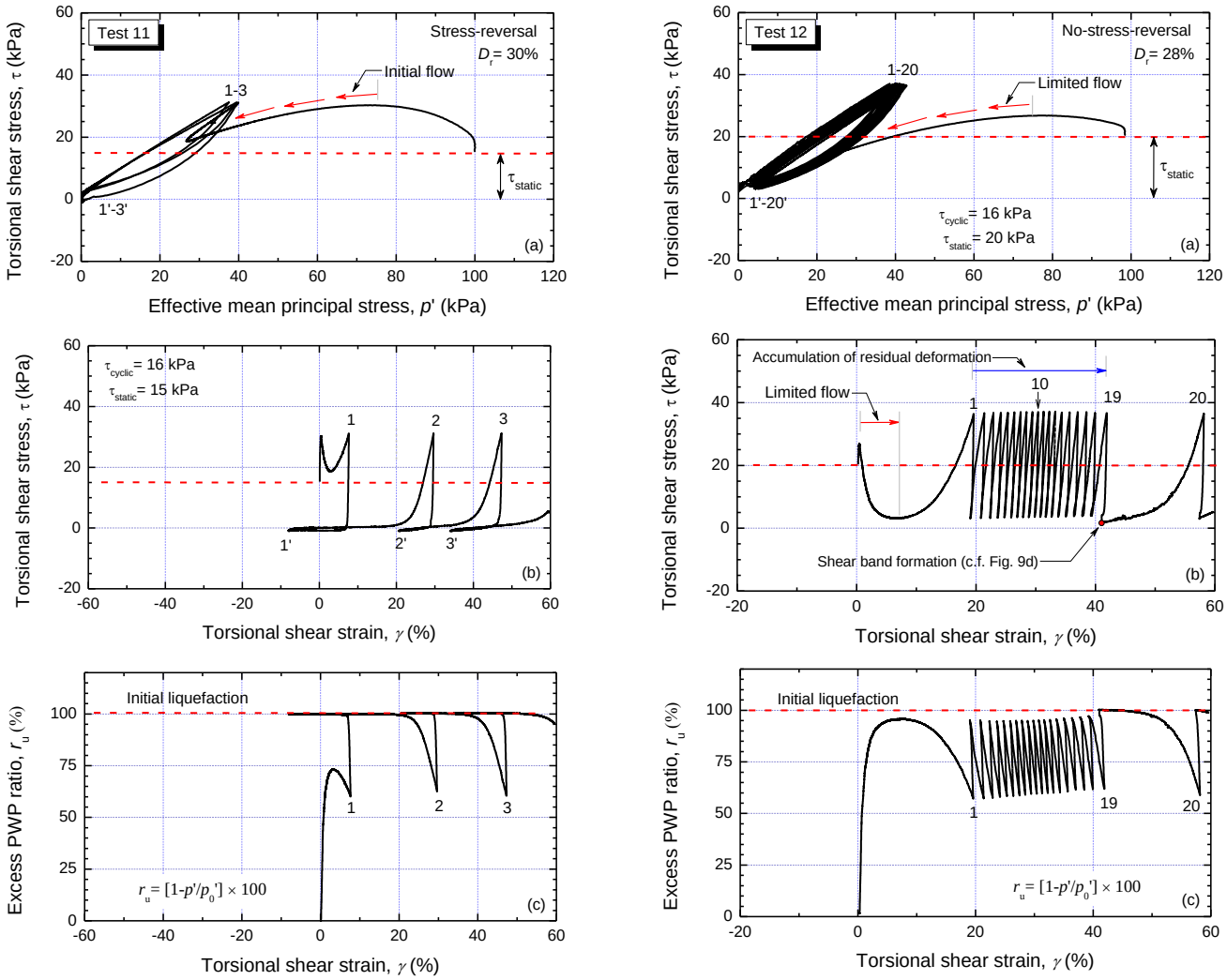

Figure 8 Rapid liquefaction response with flow deformation

This type of soil response is referred to as plastic strain accumulation (Yang and Sze, 2011a) or residual deformation failure (Chiaro et al., 2012). Under earthquake loading conditions, such an accumulation of large residual deformation would occur only if an earthquake produced a substantial number of uniform cycles with large stress amplitude, and would result into severe serviceability problems.

3.3 Cyclic Resistance of Loose and Medium Dense Sand Under Sloping Ground Conditions

A key factor to evaluate the cyclic response of liquefiable soil in level ground (τ_{static} = 0) is the resistance to cyclic strain accumulation (referred hereafter simply to as cyclic resistance), which is usually expressed as the cyclic stress ratio (CSR = τ_{cyclic}/p_0') required to develop a specific amount of double amplitude shear strain (γ_{DA}) within a given number of uniform shear stress loading cycles. When considering sloping ground, the assessment of cyclic resistance has to also account for the static shear ratio ($\alpha = \tau_{static}/p_0$').

When τ_{static} is present, γ_{DA} tends to accumulate in the loading direction where the τ_{static} is applied (i.e. it becomes unsymmetrical). Therefore, the use of single amplitude shear strain (γ_{SA}) rather than γ_{DA} has been recommended to estimate the cyclic resistance of sand under sloping ground conditions (Chiaro et al., 2012, 2013a).

The value of γ_{SA} can be expressed in terms of either the largest cyclic shear deformation of slopes during earthquakes γ_{max} (defined at $\tau = \tau_{max}$) or residual deformation of slopes just after earthquakes γ_{RS} (defined at zero cyclic shear stress, i.e. $\tau = \tau_{static;}$ Tatsuoka at al., 1982). Nevertheless, Chiaro et al. (2012) found that γ_{max} and γ_{RS} almost coincide with each other in cyclic undrained torsional shear tests, so that both can be used interchangeably.

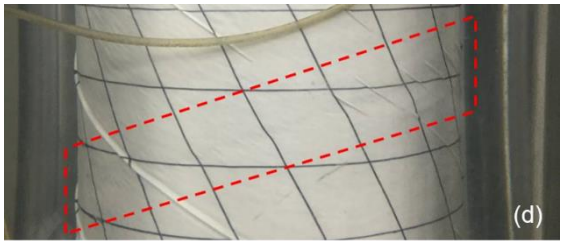

Figure 9 Accumulation of residual shear deformation with formation of shear band

In view of the above, in this paper, for any given value of α, the cyclic resistance was defined as the value of CSR to achieve γ_{max} = γ_{SA} = 7.5%, 20% and 50%. It is important to mention that although the cyclic resistance is reported for γ_{SA} = 50%, such information should be taken only as a reference since the data can be affected by strain localization (i.e. the formation of shear band) that takes place during undrained torsional shear loading (Kiyota et al., 2008; Chiaro et al., 2013a; Chiaro et al., 2015b).

The following sections discuss the effects of initial static shear, cyclic shear stress and relative density on the cyclic resisatnce of tested Toyoura sand speciemens.

3.3.1 Effect of Initial Static Shear

Figures 10 and 11 show the cyclic resistance of loose (D_r = 25-30%) and medium dense (D_r = 44-48%) Toyoura sand specimens, respectively. In Figure 12, to better capture the effects of τ_{static} on cyclic resistance, the same data are plotted also in terms of variation of cyclic resistance with α.

Evidently in the case of 7.5% the sand resistance decreases with an increase in α. At larger strains of 20% and 50%, however, the

cyclic resistance first decreases and then increases. This change in strain accumulation response can be associated with change in failure mode from cyclic liquefaction to rapid liquefaction to shear failure. Further, for any given value of α, the cyclic resistance significantly decreases with increasing *CSR*. This response is in accordance with those observed in previous studies (e.g. Hyodo et al., 1991).

3.3.2 Effect of Relative Density

In general, despite the two different levels of relative density tested in this study, Toyoura sand behavior is reasonably similar. In fact, under stress-reversal loading, a drastic drop in the cyclic resistance is observed as α increases. On the other hand, under non-stress-reversal, cyclic resistance increases with the increase in α. However, as anticipated, it is obvious that the loose sand is much weaker against cyclic strain accumulation, so that flow deformation are achieved in less number of loading cycles under the same *CSR* and α conditions.

3.4 Cyclic Resistance Ratio (*CRR*)

The cyclic resistance ratio (*CRR* = *CSR* at 10 cycles of loading; the selection of 10 cycles is consistent with the recommendation by Ishihara, 1996) versus α relationships are illustrated in Figures 13(a) and 13(b), for loose and medium dense sand specimens, respectively.

In both cases, the cyclic resistance first decrease (detrimental effect of τ_{static}) and then increases (beneficial effect of τ_{static}) upon the no-stress-reversal loading line. These results and trends are reasonable consistent with experimental results reported in the literature where the simple shear conditions were employed (e.g. direct simple shear tests by Ziotopoulou and Boulanger, 2016).

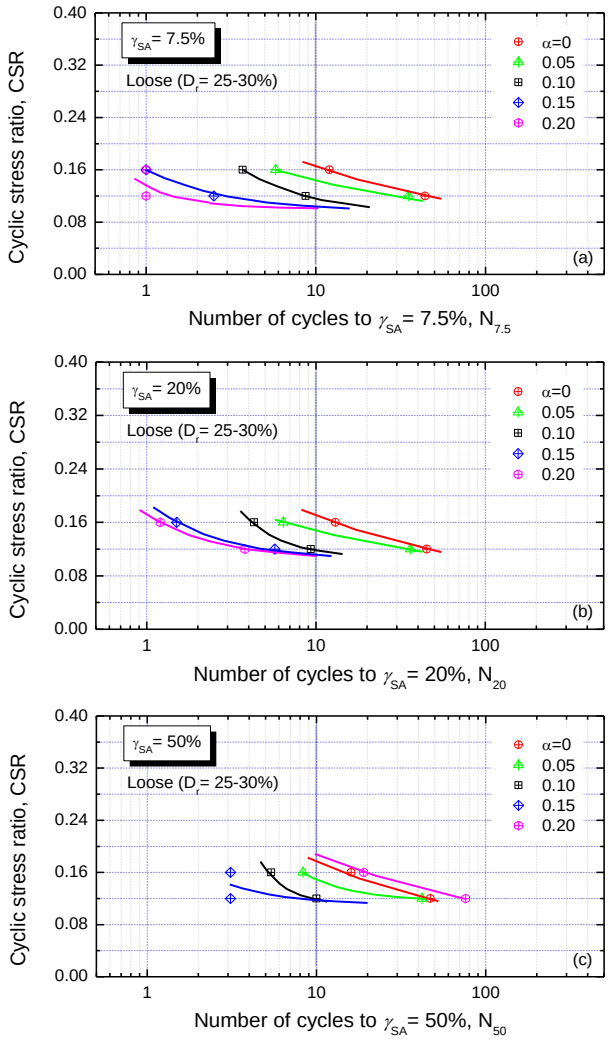

Figure 10 Cyclic resistance of loose Toyoura sand (D_r = 25-30%) under sloping ground conditions

3.5 K_α factor

The effect of α on the cyclic resistance ratio is often expressed by the K_α factor (Seed, 1983) that is defined as the ratio of CRR_α at any given α value to that of *CRR* for level ground conditions at α = 0 (i.e. $K_\alpha = CRR_\alpha / CRR_0$). The value of K_α indicates if the presence of τ_{static} is detrimental (K_α < 1) or beneficial (K_α > 1) to the sand cyclic resistance.

Figure 14 displays the variation of K_α with α obtained in this study for loose and medium dense Toyoura sand under sloping ground conditions and a mean effective stress of 100 kPa.

3.5.1 Loose Sand

Figure 14(a) shows that for loose sand the presence of τ_{static} appears to be detrimental up to α = 0.15-0.20. This is also confirmed by the failure mechanisms analysis, since in the range of α = 0-0.15, a change from cyclic liquefaction to rapid flow liquefaction behavior was observed. However, beyond α = 0.15, due to an increase of CRR_α, K_α starts to increase and eventually becomes > 1 (beneficial) for α = 0.2-0.25. This change from detrimental to beneficial can be associated with a change from rapid liquefaction with flow deformation development to shear failure with progressive accumulation of residual deformation.

3.5.2 Medium Dense Sand

In a similar manner, for medium dense sand, the presence of τ_{static} is detrimental up to α = 0.15. However, beyond this value CRR_α increases and K_α eventually becomes > 1 (beneficial) for α = 0.22.

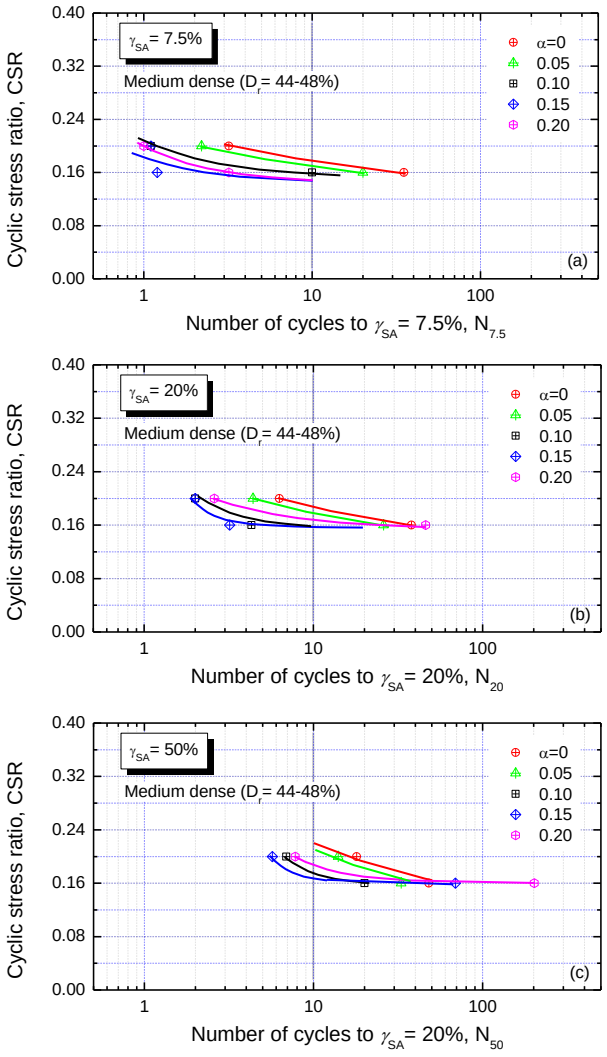

Figure 11 Cyclic resistance of medium dense Toyoura sand (D_r = 44-48%) under sloping ground conditions

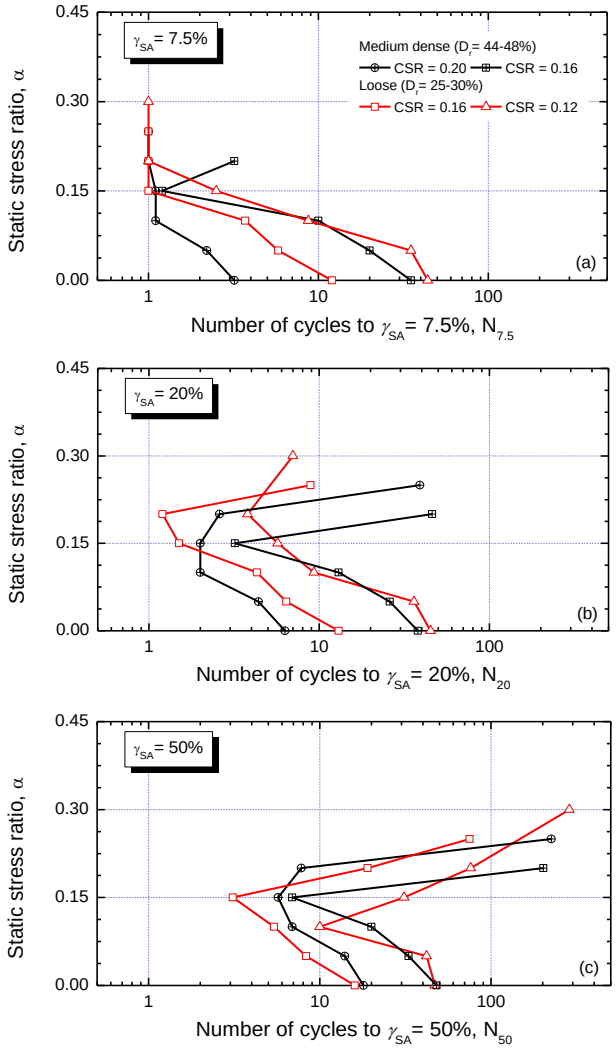

Figure 12 Cyclic resistance expressed in terms of α

3.6 Effects of Fabric on Sand Failure Modes

Laboratory observations have shown that soil fabric (i.e. spatial arrangement of sand particles and associated voids) plays an important role on sand response to cyclic loading (Ladd, 1977; Mulilis et al., 1977) and its failure modes (Sze and Yang, 2014). Therefore, the fabric should be regarded as a state parameter as important as density and stress state in describing soil behavior. However, due to the lack of a complete experimental database for hollow cylindrical Toyoura sand specimens prepared with different methods (e.g. moist tamping or water sedimentation) that would provide different soil fabric, fabric effects were not considered in this paper. This would need to be addressed by future and more comprehensive experimental studies.

4. CONCLUSIONS

In this paper, based on results of two series of large-strain undrained cyclic torsional simple shear tests with initial static shear conducted on loose and medium dense Toyoura sand specimens (relative density of 25-30% and 44-48%), an attempt was made to address the issue of earthquake-induced flow deformation response of liquefied sand subjected to sloping ground conditions. The following conclusions can be drawn from this study:

1) Under simple shear conditions, sands in sloping ground may experience three distinct failure mechanisms during earthquakes, namely cyclic liquefaction, rapid (flow) liquefaction and residual deformation failure. The most critical one is the rapid liquefaction which produces an abrupt development of large shear deformation (i.e. flow failure) without any warning. On the other hand, when the onset of initial liquefaction is not achieved, shear failure may be induced by a progressive accumulation of large residual deformation.
2) Cyclic and rapid (flow) liquefaction can only occur under stress-reversal loading conditions. In contrast, residual deformation failure may take place under no-stress-reversal loading conditions.
3) It is demonstrated that the presence of initial static shear (i.e. sloping ground conditions) can be either detrimental or beneficial to cyclic resistance. In this regard, a threshold value of α exists after which cyclic resistance of sand tends to increase with α. The α-threshold identifies the change in failure behavior between liquefaction and residual deformation failure.

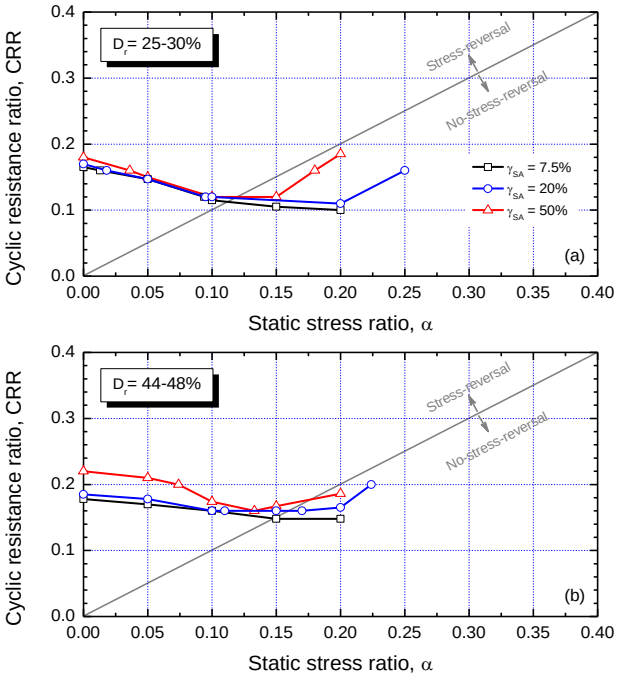

Figure 13 Cyclic resistance ratio versus α relationships

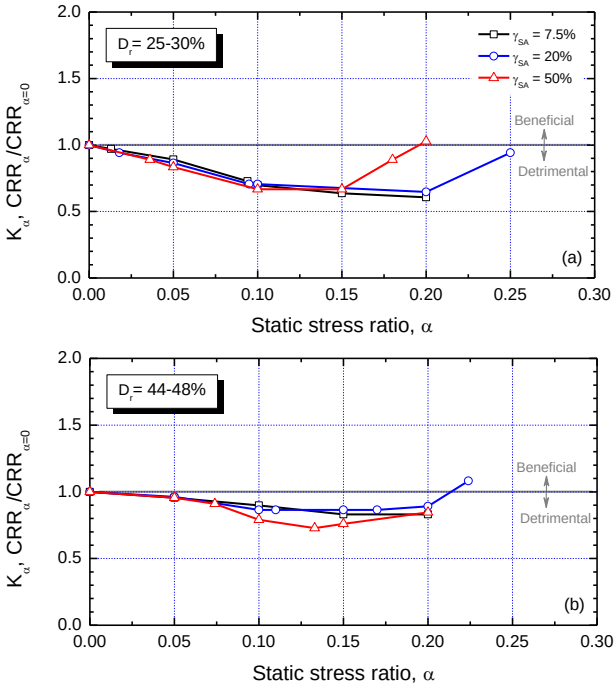

Figure 14 K_α versus α relationships

5. ACKNOWLEDGMENTS

The first Author's research at the University of Tokyo was supported by the Japanese Society for Promotion of Science Research Fellowship Award No. P14056. This support is gratefully acknowledged. Any opinions, findings, conclusions or recommendations expressed herein are those of the authors and do not necessarily reflect the views of this organization.

6. REFERENCES

Ampadu, S. I. K. (1991) "Undrained behavior of kaolin in torsional simple shear", Ph.D. Thesis, Department of Civil Engineering, University of Tokyo, Japan.

Arangelovski, G., and Towhata, I. (2004) "Accumulated deformation of sand with initial shear stress and effective stress state lying near failure conditions", Soils and Foundations, 44(6): pp1-16.

Cappellaro, C., Cubrinovski, M., Bray, J. D., Chiaro, G., Riemer, M. F., and Stringer, M. E. (2018) "Comparisons in the cyclic direct shear response of two sands from Christchurch, New Zealand", ASCE Geotechnical Special Publication, 293, pp150-159.

Castro, G. and Poulus, S. J. (1977) "Factors affecting liquefaction and cyclic mobility", Journal of the Geotechnical Engineering Division, 103(GT6), pp501-551.

Chiaro, G., Alexander, G., Brabhaharan, P., Massey C., Koseki J., Yamada, S., and Aoyagi, Y. (2017a) "Reconnaissance report on geotechnical and geological aspects of the 2016 Kumamoto Earthquake, Japan", Bulletin of the New Zealand Society for Earthquake Engineering, 50(3), pp365-393.

Chiaro, G., De Silva, L. I. N., and Koseki, J. (2017b) "Modeling the effects of static shear on the undrained cyclic torsional simple shear behavior of liquefiable sand", Geotechnical Engineering Journal, 48(4), pp1-9.

Chiaro, G., Kiyota, T., and Koseki, J. (2013a) "Strain localization characteristics of loose saturated Toyoura sand in undrained cyclic torsional shear tests with initial static shear", Soils and Foundations, 53(1), pp23-34.

Chiaro, G., Kiyota, T., and Koseki, J. (2015a) "Strain localization characteristics of liquefied sands in undrained cyclic torsional shear tests", Advances in Soil Mechanics and Geotechnical Engineering, IOS Press, Vol. 6, pp832-839.

Chiaro, G., Kiyota, T., and Miyamoto, H. (2017c), "Liquefaction potential and large deformation properties of Christchurch liquefied sand subjected to undrained cyclic torsional simple shear loading", Proceedings of 19th Int. Conf. Soil Mechanics and Geotechnical Engineering, Seoul, South Korea, pp1497-1500.

Chiaro, G., Kiyota, T., Pokhrel, R.M., Goda, K., Katagiri, T., and Sharma, K. (2015b) "Reconnaissance report on geotechnical and structural damage caused by the 2015 Gorkha Earthquake, Nepal", Soils and Foundations, 55(5), pp1030-1043.

Chiaro, G., Koseki, J., and De Silva, L. I. N. (2013b) "A density- and stress-dependent elasto-plastic model for sands subjected to monotonic torsional shear loading", Geotechnical Engineering Journal, 44(2), pp18-26.

Chiaro, G., Koseki, J., and Sato, T. (2012) "Effects of initial static shear on liquefaction and large deformation properties of loose saturated Toyoura sand in undrained cyclic torsional shear", Soils and Foundations, 52(3), pp498-510.

Chiaro, G., Umar, M., Kiyota, T., and Massey, C. (2018) "The Takanodai landslide, Kumamoto, Japan: insights from post-earthquake field observations, laboratory tests and numerical analyses", ASCE Geotechnical Special Publication, 293, pp98-111.

Cubrinovski, M., and Ishihara, K. (2000) "Flow potential of sandy soils with different grain compositions", Soils and Foundations, 40(4), pp103-119.

Cubrinovski, M., Bray, J. D., Taylor, M., Giorgini, S., Bradley, B. A., Wotherspoon, L., and Zupan, J. (2011) "Soil liquefaction effects in the Central Business Districts during the February 2011 Christchurch Earthquake", Seismological Research Letters, 82(6), pp893-904.

Cubrinovski, M., Green, R. A., Allen, J., Ashford, S. A., Bowman, E., Bradley, B. A., Cox, B., Hutchinson, T. C., Kavazanjian, E., Orense, R. P., Pender, M., Quigley, M., and Wotherspoon, L. (2010) "Geotechnical reconnaissance of the 2010 Darfield (Canterbury) Earthquake", Bulletin of the New Zealand Society of Earthquake Engineering, 42(4), pp243-320.

De Silva, L. I. N., Koseki, J, Chiaro, G., and Sato, T. (2015) "A stress-strain description for saturated sand under undrained cyclic torsional shear loading", Soils and Foundations, 55(3), pp559-574.

Georgiannou, V. N., Tsomokos, A., and Stavrou, K. (2008) "Monotonic and cyclic behaviour of sand under torsional loading", Geotechnique, 58(2), pp113-124.

Hight, D. W., Gens, A., and Symes, M. J. (1983) "The development of a new hollow cylinder apparatus for investigating the effects of principal stress rotation in soils", Geotechnique, 33, pp355-383.

Hyodo, M., Murata, H., Yasufuku, N., and Fujii, T. (1991) "Undrained cyclic shear strength and residual shear strain of saturated sand by cyclic triaxial tests", Soils and Foundations, 31(3), pp60-76.

Hyodo, M., Tanimizu, H., Yasufuku, N., and Murata, H. (1994) "Undrained cyclic and monotonic triaxial behavior of saturated loose sand", Soils and Foundations, 34(1), pp19-32.

Ishihara, K. (1996) "Soil beahviour in earthquake Geotechnics", Clarendon Press, Oxford.

Kiyota, T., Kyokawa, H., and Konagai, K. (2011) "Geo-disaster report on the 2011 Tohoku-Pacific Coast Earthquake", Bulletin of Earthquake Resistant Structure Research Center, 44, pp17-27.

Kiyota, T., Sato, T., Koseki, J., and Mohammad, A. (2008) "Behavior of liquefied sands under extremely large strain levels in cyclic torsional shear tests", Soils and Foundations, 48(5), pp727-739.

Koseki, J., Yoshida, T., and Sato, T. (2005) "Liquefaction properties of Toyoura sand in cyclic torsional shear tests under low confining stress", Soils and Foundations, 45(5), pp103-113.

Ladd, R. S. (1977) "Specimen preparation and cyclic stability of sands", Journal of the Geotechnical Engineering Division, 103(6), pp535-547.

Mulilis, J. P., Arulanandan, K., Mitchell, J. K., Chan, C. K., and Seed, H. B. (1977) "Effects of sample preparation on sand liquefaction", Journal of the Geotechnical Engineering Division, 103(2), pp91-108.

Seed, H. B. (1983) "Earthquake-resistant design of earth dams", Proceedings of Symposium on Seismic Design Earth Dams and Caverns, New York, pp41-46.

Seed, H. B., and Idriss, I. M. (1982) "Ground Motions and Soil Liquefaction during Earthquakes", Earthquake Engineering Research Institute Monograph, Oakland.

Sivathayalan, S., and Ha, D. (2011) "Effect of static shear stress on the cyclic resistance of sands in simple shear loading", Canadian Geotechnical Journal, 48(10), pp1471–1484.

Sze, H. Y., and Yang, J. (2014) "Failure modes of sand in undrained cyclic loading: impact of sample preparation", Journal of Geotechnical and Geoenvironmental Engineering, 140, pp152-169.

Tatsuoka, F., Muramatsu, M., and Sasaki, T. (1982) "Cyclic undrained stress-strain behavior of dense sands by torsional simple shear stress", Soils and Foundations, 22(2), pp55-70.

Vaid, Y. P., and Chern, J. C. (1983), "Effects of static shear on resistance to liquefaction". Soils and Foundations, 23, pp47-60.

Vaid, Y. P., and Finn, W. D. L. (1979) "Static shear and liquefaction potential", Journal of the Geotechnical Engineering Division, 105, pp1233-1246.

Vaid, Y. P., Stedman, J. D., and Sivathayalan, S. (2001): "Confining stress and static shear effects in cyclic liquefaction", Canadian Geotechnical Journal, 38(3), pp580-591.

Verdugo. R., and Ishihara, K. (1996) "The steady-state of sandy soils", Soils and Foundations, 36(2) pp81-91.

Yang, J., and Sze, H. Y. (2011a) "Cyclic behavior and resistance of saturated sand under non-symmetrical loading conditions", Geotechnique, 61(1), pp59-73.

Yang, J., and Sze, H. Y. (2011b) "Cyclic strength of sand under sustained shear stress", Journal of Geotechnical and Geoenvironmental Engineering, 137(2), pp1275-1285.

Yoshimi, Y., and Oh-oka, H. (1975) "Influence of degree of shear stress reversal on the liquefaction potential of saturated sand", Soils and Foundations, 15(3), pp27-40.

Ziotopoulou, K., and Boulanger R. W. (2016) "Plasticity modeling of liquefaction effects under sloping ground and irregular loading conditions", Soil Dynamics and Earthquake Engineering, 84: pp269-283.